Doppler-Shifted Cyclotron Resonance and Alfvén Wave Damping in Bismuth

JORDAN KIRSCH*
IBM Watson Laboratory, Columbia University, New York, New York
(Received 17 September 1963)

At large magnetic fields the transmission of microwaves through bismuth is essentially undamped and can be regarded as Alfvén waves in a solid-state plasma. A large kink has been observed in the 9-Gc/sec microwave absorption of bismuth as a perpendicularly applied magnetic field was varied through 1500 G. These experiments have been performed at 2°K with a field parallel to the binary axis. The kink has been identified as a Doppler-shifted cyclotron resonance whose position is approximately given by the formula $\omega=\omega_c-v_{0x}k_A$ where v_{0x} is the maximum Fermi velocity along the field and k_A is the wave number of the microwaves in the metal. The kink marks the onset of Alfvén wave behavior where the surface resistance is proportional to magnetic field. A calculation of the surface resistance using a nonlocal theory applied to a three-carrier model yields a variation with field which shows both the Doppler-shifted peak and the high-field linear region which can be extrapolated back through the origin. The frequency dependence of the peak derived from this calculation has been verified experimentally. By tilting the field slightly away from the perpendicular it was shown that the peak was a Doppler shift in the cyclotron resonance of the holes rather than of the electrons. This experiment provides a very accurate measure of the ratio of the Fermi velocity to the Alfvén velocity and, thus, knowing one, the other may be determined. For this reason, the Alfvén velocity in the same crystals was independently measured using an interference technique. Oscillations with a constant period in $1/H$ were observed in the reflected power as the applied magnetic field was varied. From the period of oscillation and the thickness of the crystal, the velocity was deduced. The work also provides a graphic measure of the sharpness of the Fermi surface.

I. INTRODUCTION

IT is well known that cyclotron resonance experiments in metals and semimetals yield results which are considerably different from those which are performed in semiconductors. In the latter case, the absorption demonstrates the usual resonance shape, whereas in metals it takes the form of an absorption edge which, in the limit of infinite mean free path, extrapolates to zero at the cyclotron resonance field of the heaviest carrier present.

If the metal can be characterized by a complex dielectric constant or conductivity, then the power absorbed by a surface of the metal in a microwave cavity is given by the expression:

$$\text{Abs. coeff.}=4\,\mathrm{Re}\epsilon^{-1/2}, \tag{1}$$

where

$$\epsilon=\epsilon_{\text{lattice}}+4\pi i\sigma/\omega.$$

These two equations are consequences of Maxwell's equations and Ohm's Law. In metals the first term on the right is negligible with respect to the second. The rf conductivity in the presence of a dc magnetic field is given by

$$\sigma=\sigma_0/[1+i(\omega-\omega_c)\tau], \tag{2}$$

where $\sigma_0=ne^2\tau/m^*$ is the classical dc conductivity, τ is the mean free time, $\omega_c=eH/m^*c$ is the cyclotron frequency, n is the number of carriers per cm^3, and m^* is the effective mass of the carriers. Equation (2) applies in the case of a single type of carrier. Substituting in Eq. (1) we can plot the dielectric constant (Fig. 1) as a function of magnetic field. Except near resonance the dielectric constant is real. At low fields it is negative and large, and there is nearly complete external reflection from the surface. At high fields the dielectric constant is positive, real, and large and therefore $\epsilon^{1/2}$ is real and absorption takes place. Thus the absorption at constant frequency has the form of Fig. 1, rather than the characteristic resonant form observed in semiconductors.

At larger magnetic fields the transmission of microwaves through bismuth is essentially undamped and can be regarded as Alfvén waves in a solid-state plasma.[1] For an isotropic plasma the Alfvén wave vector is given by

$$k_A=(\omega/H)\left(4\pi\sum_j n_jm_j\right)^{1/2}, \tag{3}$$

where n_j is the density of the jth plasma carrier, m_j its mass, and the summation extends over all carriers. The anisotropic case will be treated later. It will also be shown that this equation is a direct consequence of the equality of electrons and holes.

From this equation together with Eq. (1) one obtains the result that, in the high-field region, the absorption is proportional to H, as illustrated in Fig. 1.

This qualitative picture can readily be extended to the nonlocal case by including the effect of particle drift motion. A carrier moving toward the surface experiences a microwave field Doppler-shifted to a higher frequency. Thus the absorption edge will occur not merely at the cyclotron frequency but over a range of frequencies depending on the range of carrier velocities; in this case

* Present address for 1963–64: CEN Saclay, Gif-sur-Yvette (S. et O.) France.

[1] S. J. Buchsbaum and J. K. Galt, Phys. Fluids 4, 1514 (1961). When the total number of positive and negative carriers are unequal as in the case of ordinary metals, this mode of propagation is called the helicon wave.

determined by the Fermi velocity. The highest field at which damping can occur will be given by the condition

$$\omega=\omega_c-v_{0x}k_A, \tag{4}$$

where v_{0x} is the maximum velocity component along the propagation direction of the microwaves of a carrier at the Fermi surface, k_A is the Alfvén wave vector of the microwave field in the metal, and ω_c is the cyclotron frequency.

This result was suggested by the work of Haering and Miller[2] who solved the Boltzmann equation assuming specular reflection from the surface. We have applied their theory to an idealized model of bismuth.[3] The calculation will be discussed in Sec. III. A simplified plot of the results of this calculation is shown in Fig. 2. The broken line gives the absorption calculated using a local theory with a small amount of scattering. In the absence of this scattering the broken line would intersect the x axis at about 700 G, the unshifted cyclotron field. The tails of both the local and nonlocal plots have been exaggerated for clarity. Except in the region between -200 and $+1500$ G the local and the nonlocal curves are coincident.

Thus the nonlocal theory can be thought of as a Doppler-spreading of the classical resonance at 700 G. The carriers have a distribution in the average x component of drift velocity which varies from $+v_{0x}$ to $-v_{0x}$. One should expect a distribution of Doppler-shifted resonances varying from -200 to $+1500$ G. However, it is only those carriers with a nearly vanishing v_x which return to the skin depth every orbit. The others, due to their finite value of v_x, drift away from the skin depth before multiple orbits can be made. In Sec. II we show that a small inflection point at the point corresponding to the unshifted cyclotron resonance is, in fact, observed.

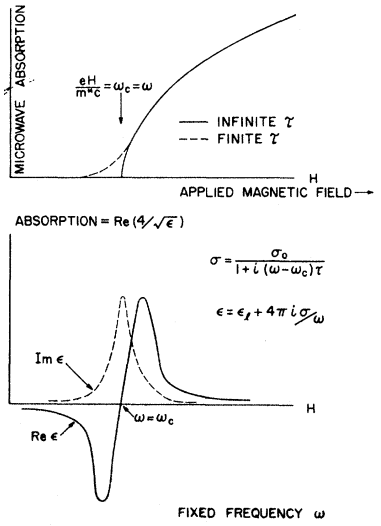

FIG. 1. Classical cyclotron absorption and dielectric constant in metals and semimetals as a function of perpendicularly applied magnetic field.

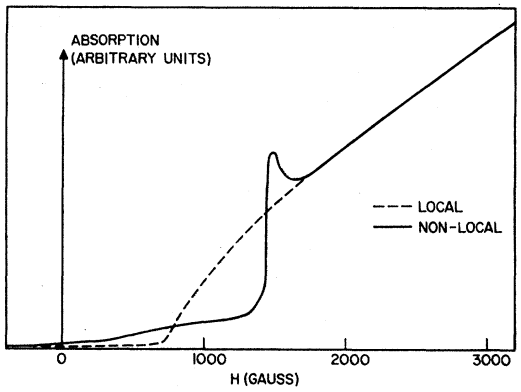

FIG. 2. Simplified theoretical plot of absorption according to local and nonlocal theories.

The large singularity at 1500 G occurs at the field satisfying Eq. (4). At this point the skin depth suddenly increases by nearly 4 orders of magnitude. To understand this, one must go back to the fundamental reason for the absorption.

There are two major mechanisms leading to damping of electromagnetic waves in a metal. The first is the dissipative effect of collisions. In materials as pure as those used in this experiment (i.e., when the mean free path is long) this effect is of secondary importance. Here the significant damping mechanism is due to energy-conserving processes in which the electrons in the metal continuously absorb both energy and momentum from the electromagnetic field.

In the presence of a dc magnetic field the momentum states of the electrons become quantized into Landau levels. As the field is increased, the spacings increase until the point is reached where the energy splitting of the levels is just equal to a quantum of the Doppler-shifted microwave field. Beyond this point the selection rules forbid any further damping due to energy-conserving processes. This point marks the onset of the nearly undamped Alfvén waves. It is at this point that the peak in Fig. 2 appears. The peak then is due to the sudden rise by several orders of magnitude of the skin depth at this point. It is a significant result of the theory that, although no assumptions about Alfvén waves were made in deriving the equations of the curve in Fig. 2, the position of the peak satisfies Eq. (4), where k_A is the wave vector of an Alfvén wave. It has previously been shown experimentally[4] that transmission of electromagnetic radiation through bismuth can be treated as Alfvén waves. The present work experimentally establishes the fact that the onset of the Alfvén region occurs precisely at the field corresponding to the Doppler-shifted cyclotron resonance of the heaviest carrier.

The use of Eq. (4) enables one to deduce directly the Fermi velocity of the carriers without employing any

[2] P. B. Miller and R. R. Haering, Phys. Rev. 128, 126 (1962).
[3] J. Kirsch and P. B. Miller, Phys. Rev. Letters 9, 421 (1962).
[4] G. A. Williams, Bull. Am. Phys. Soc. 7, 409 (1962).

model of the Fermi surface. It is however, necessary to know the Alfvén velocity. This was found by measuring the oscillations in the reflection of microwaves from the surface of the crystal in a magnetic field as the field strength was varied.[5] These oscillations were due to the standing waves in the thickness of the crystal. The method is similar to the interferometric technique of Williams.[4,6]

II. EXPERIMENTAL RESULTS

A. Doppler-Shifted Cyclotron Resonance

Figure 3 shows an experimental plot of absorption versus magnetic field. The dc field was parallel to the binary axis of the crystal and perpendicular to the surface. The temperature was 2°K and the frequency

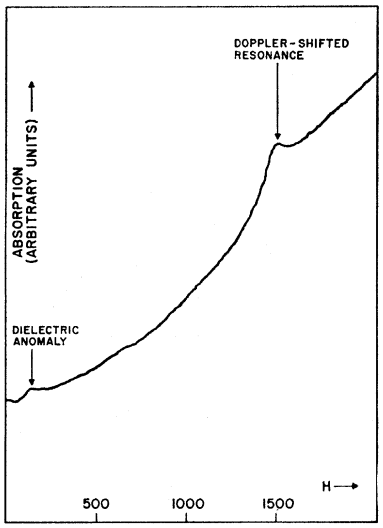

FIG. 3. Experimental plot of absorption versus H. The field was applied parallel to the binary axis and perpendicular to the surface.

9 Gc/sec. The figure shows good qualitative agreement with the calculated absorption discussed in the last section. In particular, the value of the field (1500 G) at which the peak occurs is in excellent agreement with the solution of Eq. (4). The use of field modulation and lock-in detection yields a derivative trace which, of course, exhibits far more of the structure of this plot. Figure 4 is a low-field plot of the absorption taken with the field parallel to a binary axis and perpendicular to the surface. If the experiment were performed in the usual Azbel'-Kaner geometry, three independent subharmonic series would be obtained corresponding to two different values of electron effective mass and one value of hole mass. It has been shown[7,8] that subharmonics can also be observed with the field normal as long as the plane of the orbit in real space is tilted with respect to the surface. For two of these masses, however, the field direction is parallel to a principal axis

[5] J. Kirsch, Bull. Am. Phys. Soc. 8, 205 (1963).
[6] G. A. Williams, Bull. Am. Phys. Soc. 8, 205 (1963).
[7] J. F. Koch and A. F. Kip, Phys. Rev. Letters 8, 473 (1962).
[8] G. E. Everett, Phys. Rev. 128, 2564 (1962).

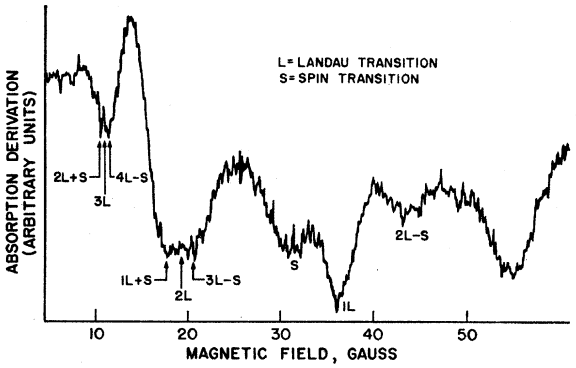

FIG. 4. Azbel'-Kaner oscillations obtained at low fields with $H \parallel$ binary axis $\perp$ surface.

of the corresponding ellipsoid and therefore, only one subharmonic series is obtained. In this trace, some of the peaks have been identified as arising from spin transitions and others from combinations spin and Landau transitions. The values of cyclotron mass for this series agrees with that obtained by Kao[9] at 24 Gc/sec.

The most interesting derivative plot is that taken with the field parallel to the binary axis and perpendicular to the surface (Fig. 5). The large peak at 125 G is the dielectric anomaly discussed by Galt[10] and others. Below this field, the beginning of a good Azbel'-Kaner series for the light electron is discernible. The latter was identified on earlier runs in which the low-field region was swept through much more slowly. At 450 and 707 G there are two small peaks which we believe correspond to the unshifted heavy electron and hole, respectively, as explained in Sec. I. The most significant feature of this curve, however, is the very large resonance at 1500 G corresponding to the peak in Fig. 1. This peak represents the Doppler-shifted cyclotron resonance of the holes in the binary direction and occurs at the point at which there is a sudden enormous increase in the skin depth.

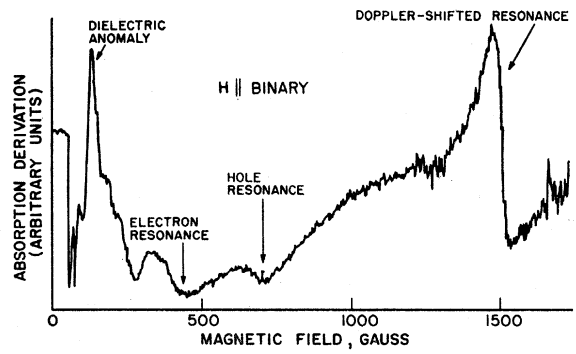

FIG. 5. Derivation of absorption versus H. $H \parallel$ binary axis $\perp$ surface.

[9] Y. H. Kao, Phys. Rev. 129, 1122 (1963).
[10] J. K. Galt, W. A. Yager, F. R. Merritt, B. B. Cetlin, and A. D. Brailsford, Phys. Rev. 114, 1396 (1959).

Of course, the possibility that the high-field peak is actually due to a "simple" or unshifted cyclotron resonance of a heavier, previously unreported, carrier must be considered. If this were the case the resonant field H_c would be proportional to the applied frequency. The two straight lines in Fig. 6 show the expected frequency dependence for two carriers: the well-known hole of mass approximately $0.225m_0$ and a heavier hypothetical carrier of mass sufficient to explain the 1500 G peak as a simple resonance. The cross marks the observed point at 1500 G and 9 Gc/sec. Also plotted is Eq. (4).

$$\omega=\omega_c-v_{ox}k_A$$
$$=\left(\frac{e}{m^*c}\right)H-\frac{v_{ox}\omega(4\pi\sum_j n_jm_j)^{1/2}}{H}, \qquad (4)$$

where m^* has been chosen $=0.225m_0$. It was impossible to check this dependence except in the limited region between 8 and 10 Gc/sec. Within this narrow range the

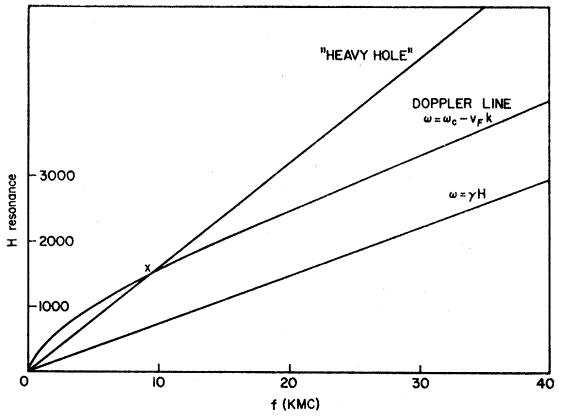

FIG. 6. Theoretical plots of resonant fields versus frequency. Cross marks region of this experiment.

frequency dependence is approximately linear and, therefore, it is best checked by comparing slopes. Figure 7 is an expanded picture of the experimental region. It appears that the experimental curve does not extrapolate through the origin and, therefore, cannot correspond to a simple unshifted cyclotron resonance.

The frequency dependence also helps to explain why this effect has not been reported before. Most cyclotron resonance experiments in bismuth have been performed at higher frequencies (generally 24, 36, or 72 Gc/sec) for which the effect is predicted to decrease. Then too, one would not expect to observe this effect while performing an experiment with H parallel to the surface since the average drift velocity in this case is parallel to the surface.

Since circularly polarized radiation cannot easily distinguish holes and electrons when they are anisotropic, linear polarization was used in this experiment. However, a field-tilting experiment was used to help to

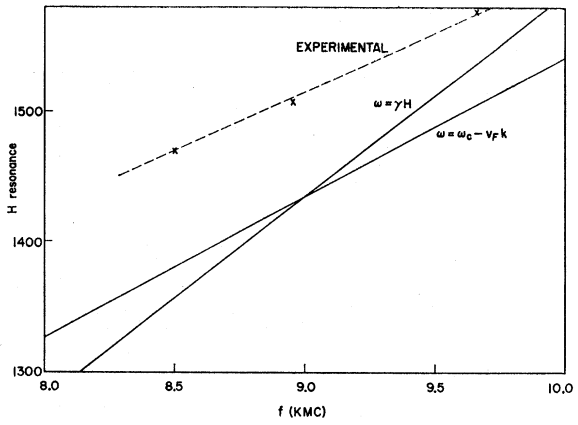

FIG. 7. Expanded plot of the region around the cross in Fig. 6.

identify the kink at H_c as due to holes. Tilting the field away from the normal to the surface toward the bisectrix direction produced virtually no change in H_c. Tilting toward the trigonal axis produced a fairly large variation in H_c. The results of both of these experiments are plotted in Fig. 8.

The hole ellipsoid has rotational symmetry about the trigonal axis and hence neither its effective mass nor its component of the Fermi velocity along H varies as H is tilted toward the bisectrix. On the other hand, as the field is tilted toward the trigonal direction both m^* and v_F vary strongly since the latter direction is a major axis of a long thin ellipsoid. If the resonance were due to the heavy electrons, the two cases would be reversed since the electron ellipsoid is also long and thin with a major axis nearly perpendicular to that of the hole ellipsoid.

Although the theory correctly predicts the stronger angular dependence of H_c for tilts in the trigonal direction than for tilts in the bisectrix, the almost complete absence of variation of H_c in the latter case is somewhat surprising. It will be shown in the next section that the Alfvén wave number k_A decreases as the tilt angle is increased in either direction. Like the other quantities in Eq. (4), k_A varies more strongly as the field is tilted toward the trigonal than as it is tilted

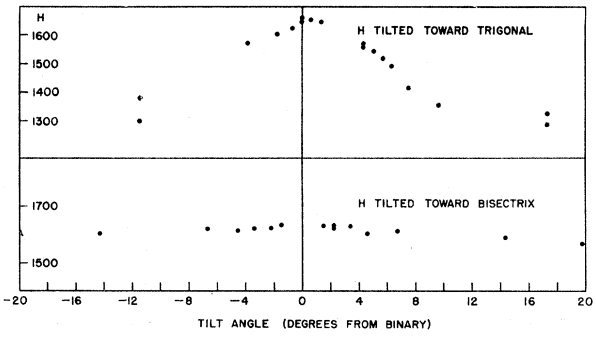

FIG. 8. Resonant field H_c as a function of tilt angle.

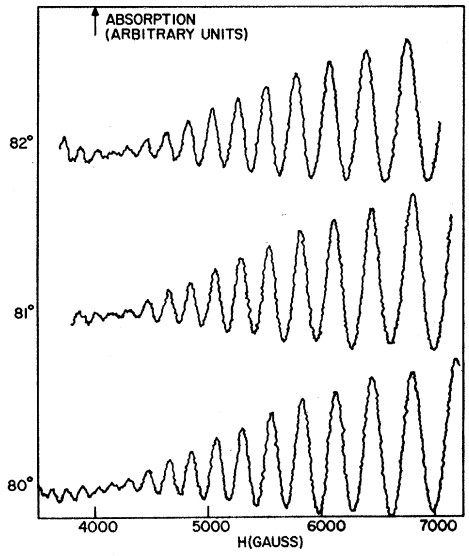

FIG. 9. X-Y recorder trace of absorption versus H. Angles refer to tilt angle between H and surface normal.

toward the bisectrix. All of this tends to support the argument that the resonance is due to holes and not electrons, but leaves unanswered the question of very small angular variation in the bisectrix direction.

B. Alfvén Wave Velocity

When the dc magnetic field was swept through values several times larger than the cyclotron field, oscillations in the absorption were observed. Figure 9 shows a typical x-y recorder trace of absorption versus dc magnetic field. The angles refer to the tilt angles described below. In these runs the fields were swept up to about 7500 G. The oscillations help to verify a theoretical result of an earlier paper[3] which stated that the onset of Alfvén wave propagation should occur at the Doppler-shifted cyclotron resonance of the heaviest carrier present. The unshifted cyclotron resonance of the heaviest carrier occurs at about 700 G, the shifted resonance at about 1500 G, and the point at which the oscillations are lost in the noise is about 1900 G. If the reciprocal of the fields at which peaks occurred is plotted against successive integers, a straight line is obtained.

Equation (3) may be written as

$$k_A=(\omega/H)(4\pi nm_0)^{1/2}A\,, \tag{5}$$

where m_0 is the free electron mass and A depends not only upon the elements of the effective mass tensor, but also upon the relative orientation of the normal to the surface, the dc magnetic field, the rf polarization, and the crystallographic axes. If this equation is substituted into the standing-wave maxima condition

$$\tfrac{1}{2}N\lambda=d \tag{6}$$

the period in $1/H$ is obtained:

$$\Delta(1/H)=[2fd(4\pi nm_0)^{1/2}A\,]^{-1}, \tag{7}$$

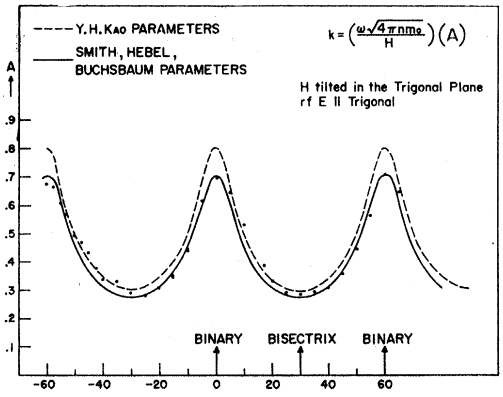

FIG. 10. The quantity A in Eq. (5) versus the angle θ between H and the normal (binary) direction. The field is tilted toward the bisectrix axis. The dots are experimental points.

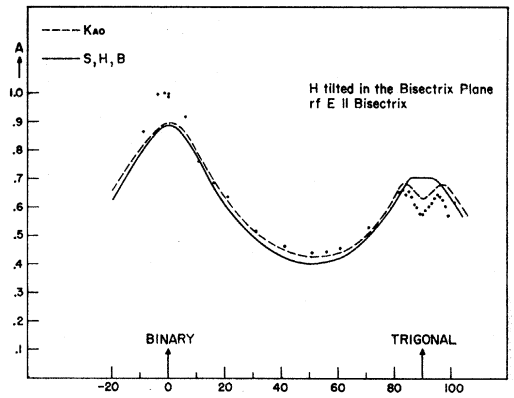

FIG. 11. The quantity A in Eq. (5) versus the angle θ between H and the normal (binary) direction. The field is tilted toward the trigonal axis. The dots are experimental points.

where f is the microwave frequency and d is the thickness of the sample. The inverse frequency dependence was verified by constructing three cavities, two of which resonated at the extremes of the X band, and the third at the center of the band. The thickness of the sample was varied from 0.1 to 1 cm.

Most of the work in this experiment was performed on crystals in which the binary axis was normal to the surface. A series of experiments was performed in which the dc magnetic field was tilted away from the normal by amounts varying from 0° to 90°. The results for the case where the field is tilted toward the bisectrix axis are shown in Fig. 10. In Fig. 11 the field was tilted toward the trigonal axis. In both cases the ordinate is the quantity A in Eq. (5) and the abscissa is the tilt angle away from the binary axis. The solid lines give the computed variation according to various models and will be discussed in the next section.

III. THEORY

In the anomalous skin effect region, a local relation such as Ohm's law is no longer valid. The current density at a point is not simply related to the conductivity and electrical field strength at that same point but to some suitable integral of $\boldsymbol{\sigma}$ and $\mathbf{E}$ over all points in space. One can convert from the space domain to the frequency domain by Fourier-analyzing, defining the wave-number dependent conductivity by

$$\mathbf{J}(k)=\boldsymbol{\sigma}(k)\mathbf{E}(k). \tag{8}$$

Miller and Haering[2] have considered cyclotron resonance of a single isotropic carrier with the field perpendicular to the surface. We have extended their calculation to the case of three carriers (a light electron, a heavy electron, and a hole) appropriate to the case of bismuth with the field along the binary direction. They considered an incident wave circularly polarized in the yz plane and the semi-infinite metal occupying the space $x<0$. (The choice of circular polarization simplifies the calculation without essentially changing the results.) The surface impedance which is defined as

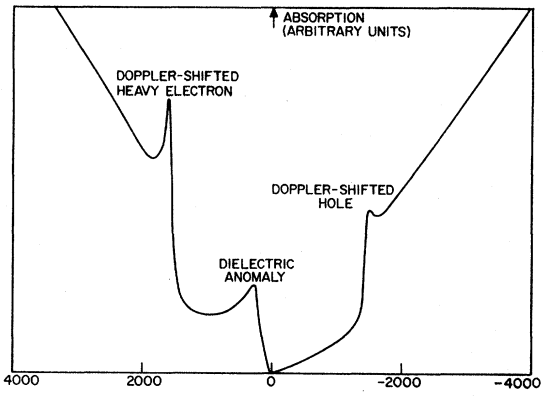

FIG. 12. Theoretical plot of absorption versus magnetic field.

$$Z=(4\pi/c)[E_y(0)/H_z(0)] \tag{9}$$

may be expressed in terms of the components of the conductivity tensor as

$$Z=\frac{8i\omega}{c^2}\int_0^\infty \frac{dk}{k^2+(4\pi i\omega/c^2)\sum_j \sigma_+^{(j)}(k)}. \tag{10}$$

The conductivity tensor for a single species of carrier in a magnetic field may be found from the Boltzmann equation:

$$\sigma_+^{(j)}=\sigma_{yy}-i\sigma_{yz}$$
$$=\tfrac{3}{4}\sigma_0^{(j)}\int_{-1}^{1}\frac{du(1-u^2)}{1+i(\omega+\omega_c^{(j)}+kv_{ox}^{(j)}u)\tau}. \tag{11}$$

The model used in our calculation was a very idealized one. No attempt was made to include the effects of anisotropy. The masses used to determine the cyclotron frequencies were those measured in this experiment and were in agreement with similar data in the literature. They are functions only of those components of the (diagonalized) effective mass tensor in a plane perpendicular to the magnetic field. The components of the Fermi velocity in the x direction were obtained from

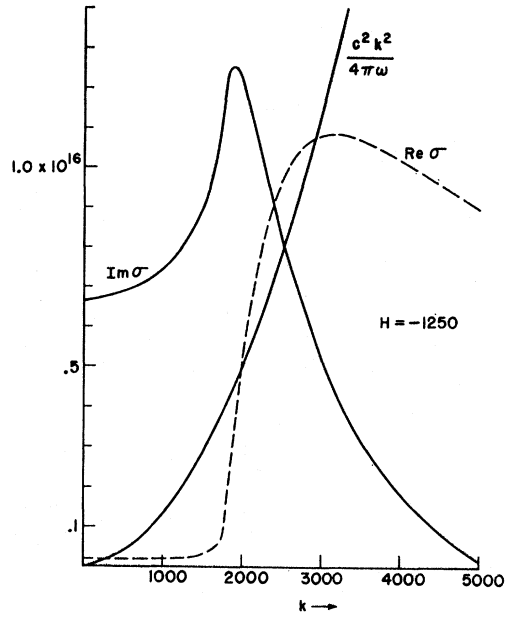

FIG. 13. The three terms in the denominator of Eq. (14) are plotted versus k. The field is 1250 G.

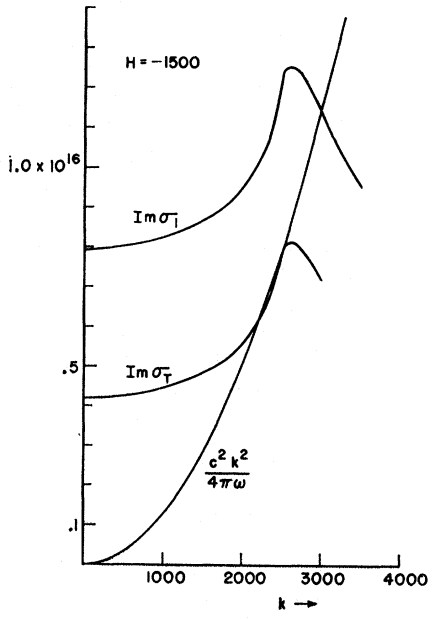

FIG. 14. $\mathrm{Im}\sigma_T$ and $c^2k^2/4\pi\omega$ are plotted versus k for a field $H_e=1500$ G. $\mathrm{Im}\sigma_l$ is explained in the text.

formulas derived below. Here, it is only the mass component in the direction of the magnetic field which enters.

Thus, the model used is equivalent to replacing the three electron and one hole ellipsoids by three spheroids with axes all in the binary direction. For each carrier the diameter is related to the cyclotron mass of that particular carrier while the height is related to the maximum Fermi velocity component in the binary direction.

Since the binary axis is a principal axis of both the hole and heavy electron ellipsoids the maximum Fermi velocities in this direction are simply: $v_{0x}=(2E_F/m_{11})^{1/2}$, where E_F and m_{11} for the holes and for the electrons were taken from the paper by Jain and Koenig.[11]

The light-electron cyclotron resonances arise from orbits on the two ellipsoids whose axes are rotated $\pm 120°$ about the trigonal axis. All the ellipses formed by the intersection of planes perpendicular to H and the ellipsoids give rise to identical values of cyclotron mass but, of course, different values of Fermi velocity. The maximum value of Fermi velocity in the x direction comes from the vanishingly small orbit at the point at which a yz plane is just tangent to the ellipsoid.

The velocity of the electrons at this point on the Fermi surface is easily calculated for this orientation:

$$v=\left[\frac{2E_F}{m_0}\left(\frac{\alpha_1'}{1+3\alpha_1'/\alpha_2'}+\alpha_2'-\frac{\alpha_2'}{1+3\alpha_1'/\alpha_2'}\right)\right]^{1/2}, \quad (12)$$

where the primed coordinated denote the elements of the diagonalized reciprocal mass tensor. The final parameter to be put into Eq. (11) is the mean free time. This has been chosen somewhat arbitrarily to be

$$\tau=0.3\times 10^{-9}\ \text{sec}. \quad (13)$$

The mean free path affects only the sharpness of the peak, not its position nor the general form of the curve away from resonance. The numerical integration was done on an IBM 7090. The results are shown in Fig. 12. Before going on to a physical discussion of this plot it might be useful to consider the mathematical origin of one of its major characteristics, the peak at 1500 G. The imaginary part of the rationalized integrand of Eq. (10) may be written as

$$\mathrm{Im}I=\frac{\mathrm{Re}\sigma}{(\mathrm{Im}\sigma-c^2k^2/4\pi\omega)^2+(\mathrm{Re}\sigma)^2}. \quad (14)$$

The three terms in the denominator are plotted in Fig. 13 for a field of 1250 G. As k approaches zero the real and imaginary parts approach their classical values:

$$\mathrm{Re}\sigma=\frac{\sigma_0}{1+(\omega-\omega_c)^2\tau^2}, \quad (15)$$

$$\mathrm{Im}\sigma=\frac{\sigma_0(\omega-\omega_c)\tau}{1+(\omega-\omega_c)^2\tau^2}. \quad (16)$$

[11] A. L. Jain and S. H. Koenig, Phys. Rev. 127, 442 (1962).

The integrand is sharply peaked about the point where $\mathrm{Im}\sigma$ crosses $c^2k^2/4\pi\omega$. The width of this peak increases as the angle of intersection decreases. Figure 14 contains plots of $\mathrm{Im}\sigma$ (labeled $\mathrm{Im}\sigma_T$) and $c^2k^2/4\pi\omega$ for a field of 1500 G, corresponding to the peak in the curve in Fig. 12. (For simplicity, the plot of $\mathrm{Re}\sigma$ has been omitted. The plot labeled $\mathrm{Im}\sigma_1$, will be explained below.) One immediately sees the reason for the peak in Fig. 12. It corresponds to the field for which the two functions are nearly tangent over a fairly large range of k values. Thus the integrand is a broad peak, having a contribution over this whole range and the integral is a maximum.

$\mathrm{Im}\sigma_1$ has been computed from Eq. (11) assuming only one carrier, the hole. One need only change the magnetic field a small amount to get $c^2k^2/4\pi\omega$ to be tangent to $\mathrm{Im}\sigma_1$. In fact, the entire calculation has been repeated for a one-carrier theory and a very similar peak occurs at 1580 G. This is the simplified curve (Fig. 2) discussed in the first section.

Nonetheless, even though the resonant field is not strongly dependent upon the number of carriers that goes into the theory, the charge cancellation resulting from the three carriers is an essential part of the theory in the high-field region.

The local theory neglects the Doppler effect. That this is the only difference between the two theories is seen by referring to Eq. (11). The classical, or local, conductivity is obtained evaluating the integral when $k=0$ but one easily sees that this is completely equivalent to evaluating the integral with $v_F=0$ or in other words, neglecting the Doppler effect.

The sharper peak at $+1600$ G is due to the Doppler-shifted heavy electron. This has not been observed. The small peak at a low field is the previously mentioned dielectric anomaly.

We turn now to a calculation of the Alfvén wave velocity for an anisotropic effective mass. From Maxwell's equations (neglecting displacement currents) one obtains

$$\nabla^2\mathbf{E}=(4\pi i\omega/c^2)\boldsymbol{\sigma}\mathbf{E}, \quad (17)$$

where $\boldsymbol{\sigma}$ is the conductivity tensor and includes the effect of magnetic field. Strictly speaking, of course, for a complete nonlocal theory, the conductivity tensor should be written $\boldsymbol{\sigma}(k)$ but we have replaced $\boldsymbol{\sigma}(k)$ by the local limit $\boldsymbol{\sigma}(0)$. At high fields this has been shown to be a good approximation. Using the definition

$$\mathbf{K}=(4\pi i\omega/c^2)\boldsymbol{\sigma}, \quad (18)$$

we get, for a field in the x direction and the surface in the y-z plane,

$$\begin{aligned} 0&=\mathrm{K}_{11}E_x+\mathrm{K}_{12}E_y+\mathrm{K}_{13}E_z,\\ \partial^2E_y/\partial x^2&=\mathrm{K}_{21}E_x+\mathrm{K}_{22}E_y+\mathrm{K}_{23}E_z,\\ \partial^2E_z/\partial x^2&=\mathrm{K}_{31}E_x+\mathrm{K}_{32}E_y+\mathrm{K}_{33}E_z. \end{aligned} \quad (19)$$

By substituting $E_y(x)=E_y(0)e^{-ikx}$ and $E_z(x)=E_z(0)$

$\times e^{-ikx}$, we can solve the secular equation for two values of k corresponding to the two normal modes:

$$k_{1,2}^2=\frac{-K_{22}-K_{33}}{2}\pm\left[\left(\frac{K_{22}-K_{33}}{2}\right)^2+K_{23}K_{32}\right]^{1/2}. \quad (20)$$

Making use of Eq. (18), we can rewrite this as

$$k_{1,2}^2=\frac{4\pi i\omega}{c^2}\left\{\frac{-\sigma_{22}-\sigma_{33}}{2}\pm\left[\left(\frac{\sigma_{22}-\sigma_{33}}{2}\right)+\sigma_{23}\sigma_{32}\right]^{1/2}\right\}. \quad (21)$$

We see that the problem is reduced to that of finding the elements of the conductivity tensor. These can be derived from the equation:

$$\mathbf{m}\frac{d\mathbf{v}}{dt}+\frac{e\mathbf{H}}{m_0c}\times\mathbf{v}+\frac{\mathbf{mv}}{\tau}=\frac{e\mathbf{E}}{m_0}. \quad (22)$$

Consider the case of bismuth with a large magnetic field parallel to the binary axis and infinite τ. One obtains, for the electrons,[12]

$$\begin{aligned}
\frac{\sigma_{11}}{\sigma_{oe}}&=\frac{1}{3m_1}+\frac{8}{3(m_1+3m_2)},\\
\frac{\sigma_{22}}{\sigma_{oe}}&=\frac{1}{b^2}\left[m_3-\frac{2m_4^2}{(m_1+3m_2)}\right],\\
\frac{\sigma_{33}}{\sigma_{oe}}&=\frac{1}{b^2}\left[\frac{m_2}{3}+\frac{8m_1m_2}{3(m_1+3m_2)}\right],\\
\frac{\sigma_{23}}{\sigma_{oe}}&=-\frac{\sigma_{32}}{\sigma_{oe}}=\frac{1}{b},
\end{aligned} \quad (23)$$

where the m's are elements of the electron effective mass tensor expressed in units of the free electron mass m_0, $\sigma_{0e}=n_e e^2/i\omega m_0$, and $b=i|e|H/m_0c\omega=i(\omega_c)_0/\omega$. Here, we have already applied the high-field condition: $b\gg m_i$. For the holes, one obtains

$$\begin{aligned}
&\sigma_{11}/\sigma_{0h}=1/M_1,\\
&\sigma_{22}/\sigma_{0h}=(1/b^2)(M_3),\\
&\sigma_{33}/\sigma_{0h}=(1/b^2)(M_1),\\
&\sigma_{23}/\sigma_{0h}=-\sigma_{32}/\sigma_{0h}=-1/b,
\end{aligned} \quad (24)$$

where $\sigma_{0h}=n_h e^2/i\omega m_0$ and the M's are elements of the hole mass tensor. n_e and n_h are the densities of electrons and holes, respectively.

It is interesting to consider first the case of electrons only, which is typical of most metals. Then, of the four conductivity terms in Eq. (21), two are proportional to b^{-1} and two to b^{-2}. Thus in the high-field case the latter terms will be negligible with respect to the former and one obtains

$$k^2=4\pi ne\omega/cH.$$

Waves of this form are called helicons[13] and have the property that the velocity is proportional to $H^{1/2}$.

Let us return to the actual case of bismuth. Here, although

$$(\sigma_{23})_{\text{electron}}\gg(\sigma_{22})_{\text{electron}},\quad(\sigma_{33})_{\text{electron}}$$

and

$$(\sigma_{23})_{\text{hole}}\gg(\sigma_{22})_{\text{hole}},\quad(\sigma_{33})_{\text{hole}}$$

the total number of electrons equals the total number of holes and thus,

$$(\sigma_{23})_{\text{total}}=(\sigma_{23})_{\text{electron}}+(\sigma_{23})_{\text{hole}}=0.$$

Consequently it is only the diagonal elements which enter into Eq. (21) and we have a very different physical case. The two normal modes are given by

$$k_1=\frac{\omega}{H}(4\pi nm_0)^{1/2}\left\{m_3+M_3-\frac{2m_4^2}{m_1+3m_2}\right\}$$

and

$$k_2=\frac{\omega}{H}(4\pi nm_0)^{1/2}\left\{M_1+\frac{m_2}{3}+\frac{8m_1m_2}{3(m_1+3m_2)}\right\}.$$

These modes are Alfvén modes and are the ones observed in this experiment. Here, k_1 corresponds to a linearly polarized mode with the rf E field parallel to the bisectrix axis and k_2 corresponds to the rf E field parallel to the trigonal axis. The quantities in the brackets are the dimensionless proportionality constants represented by A in Eq. (5).

Alfvén waves do not necessarily propagate only along the field direction. As the field direction is tilted away from the direction of propagation (the latter remaining perpendicular to the surface) the velocities of the two modes change. The expressions for A become increasingly complex. Finally when H is parallel to the surface, the quantity A for one of the modes becomes infinite (the velocity vanishes) and there remains only one propagating mode. The remaining mode is polarized perpendicular to the magnetic field.

The results of a numerical calculation of A as H is tilted away from the binary toward the bisectrix are plotted in Fig. 10. Only the mode which remains finite at $\theta=90°$ is plotted. The broken line gives the angular dependence of A using the parameters published by Kao,[9] the solid line using the parameter of Smith, Hebel, and Buchsbaum.[14] The points are the values of A measured in this experiment assuming a density of carriers[6] equal to 3.0×10^{17} cm^{-3}.

The results of the same calculations and measurements for the case of H tilted toward the trigonal axis are plotted in Fig. 11.

The fit to both of these models is quite good and it

[12] B. Lax, K. J. Button, H. J. Zeiger, and L. Roth, Phys. Rev. **102**, 715 (1956).

[13] P. Aigrain, in *Proceedings of the International Conference on Semiconductor Physics, Prague, 1960* (Czechoslovak Academy of Sciences, Prague, 1961).

[14] G. E. Smith, L. C. Hebel, and S. J. Buchsbaum, Phys. Rev. **129**, 154 (1963).

might be difficult to use an experiment of this type to distinguish between them. However, there is one characteristic of Fig. 11 which fits Kao's model much better than that of Smith, Hebel, and Buchsbaum. That is the dip when H is near the trigonal axis. The experimental points clearly show this dip and so does the broken theoretical curve. The maxima are separated from the minimum by about 5°, equal to the tilt angle of the electron ellipsoids. There is an extremely small dip predicted for the solid curve at 90°, but it is less than the thickness of the line and has not been plotted.

IV. EXPERIMENTAL METHOD

The absorption was studied in single crystals of bismuth that formed part of the walls of X-band cavities. Both cylindrical TE_{111} and rectangular TE_{102} cavities were used. In the former case the dc magnetic field was provided by a solenoid wound coaxial with the cavity. For the tilted-field experiment a Helmholtz pair was added in series with the solenoid permitting the field to be tilted up to a maximum of 20 deg. The rectangular cavity was used in conjunction with a Varian magnet. By rotating the cavity within the Dewar it was possible to tilt the field a full ±90° from the normal. The absorption was detected with the use of a microwave bridge employing a magic tee. For some of the runs, field modulation and lock-in detection were used. The temperature was reduced below the lambda point by pumping in order to reduce the noise due to bubbling. The crystals were grown in air, x-ray oriented, spark-cut and spark-planed, and finally either chemically polished or electropolished.

V. CONCLUSIONS

The most significant result of this work is the experimental verification of the necessity of using a nonlocal theory to describe completely the phenomenon of cyclotron resonance. Equation (4) provides the connection between cyclotron resonance and Alfvén wave propagation. The measured Doppler shift is directly related to the ratio of the Fermi velocity of the holes to the Alfvén velocity. The latter was measured directly at fields which varied from approximately 30% larger than the resonance field to those about five times greater than the resonance field. Experimental values of the Alfvén wave number k_A, the hole effective mass, and the applied frequency were combined with the Fermi velocity of the hole in the binary direction derived from the expression $v_F=(2E_F/m_{11})^{1/2}$ using published parameters.[11] The results are a predicted Doppler-shifted resonant field of 1380 G for the case where the rf field is polarized along the trigonal direction and 1320 G when the rf is polarized along the bisectrix direction. The observed resonant fields corresponding to these two cases were 1530 and 1465 G, respectively.

The quantitative accuracy of Eq. (4) can be estimated by substituting in it the same effective masses and Fermi energy which were used in the nonlocal integral illustrated in Fig. 12. With these values Eq. (4) predicts a Doppler-shifted resonance at 1225 G, approximately 250 G below that predicted by the more complete theory. Thus the discrepancy is in the same direction and about the same size as that between the field predicted by substitution of an independently measured value of k_A into Eq. (4) and the experimentally observed resonant field. The use of k_A in Eq. (4) is equivalent to extrapolating the linear absorption region in Fig. 12 all the way back to the peak at 1500 G. Presumably, the discrepancy is due to the fact that this extrapolation is not completely valid.

An original objective of this work had been the independent measurement of the Fermi velocity. If Eq. (4) is solved for v_{0x} with experimental values substituted for all other quantities, one obtains for the Fermi velocity of the holes in the binary direction

$$v_F=3.4\times10^7 \text{ cm/sec}.$$

The fractional difference between this number and the velocity given by the ellipsoidal model,

$$v_F=(2E_F/m_{11})^{1/2}=2.5\times10^7 \text{ cm/sec},$$

is considerably greater than the fractional discrepancy between predicted and observed resonant fields. Because of the above argument it is not surprising that this somewhat limits the usefulness of this method for determining v_F.

ACKNOWLEDGMENTS

The author would like to thank A. G. Redfield for valuable suggestions throughout the course of this work and for his sponsorship of some of this work as part of a Columbia University thesis. The author would also like to thank P. B. Miller, S. H. Koenig, and Y. H. Kao for helpful discussions.